
Tarawa Atoll

Chapter 6
Kiribati

The contributions of Ueneta Toorua, Tebwaau Tetabo and Tareti Kireua from the Kiribati Meteorology Service and Riibeta Abeta and Nakibae Teuatabo from the Environment and Conservation Division are gratefully acknowledged

Introduction

This chapter provides a brief description of Kiribati, its past and present climate as well as projections for the future. The climate observation network and the availability of atmospheric and oceanic data records are outlined. The annual mean climate, seasonal cycles and the influences of large-scale climate features such as the Intertropical Convergence Zone and patterns of climate variability (e.g. the El Niño-Southern Oscillation) are analysed and discussed. Observed trends and analysis of air temperature, rainfall, extreme events, sea-surface temperature, ocean acidification, mean and extreme sea levels are presented. Projections for air and sea-surface temperature, rainfall, sea level, ocean acidification and extreme events for the 21st century are provided. These projections are presented along with confidence levels based on expert judgement by Pacific Climate Change Science Program (PCCSP) scientists. The chapter concludes with summary tables of projections for the Gilbert, Phoenix and Line Islands (Tables 6.4, 6.5, 6.6). Important background information, including an explanation of methods and models, is provided in Chapter 1. For definitions of other terms refer to the Glossary.

6.1 Climate Summary

6.1.1 Current Climate

- Kiribati has a hot, humid tropical climate, with air temperatures very closely related to the sea-surface temperature of the surrounding oceans.
- The South Pacific Convergence Zone and the Intertropical Convergence Zone influence Kiribati's wet seasons. The driest and wettest periods in the year vary from location to location.
- High year-to-year variability in rainfall is mostly due to the impact of the El Niño-Southern Oscillation.
- Warming trends are evident in both annual and seasonal mean air temperatures at Tarawa for the period 1950–2009.
- The sea-level rise near Kiribati measured by satellite altimeters since 1993 ranges from 1–4 mm per year.
- The Kiritimati positive annual rainfall trend for the period 1950–2009 is statistically significant; however seasonal trends over the same period are not. Annual and seasonal rainfall trends for Tarawa for 1950–2009 are not statistically significant.
- Droughts, usually associated with La Niña events, are occasionally very severe in Kiribati.

6.1.2 Future Climate

Over the course of the 21st century:

- Surface air temperature and sea-surface temperature are projected to continue to increase (*very high* confidence).
- Annual and seasonal mean rainfall is projected to increase (*high* confidence).
- The intensity and frequency of days of extreme heat are projected to increase (*very high* confidence).
- The intensity and frequency of days of extreme rainfall are projected to increase (*high* confidence).
- The incidence of drought is projected to decrease (*moderate* confidence).
- Ocean acidification is projected to continue (*very high* confidence).
- Mean sea-level rise is projected to continue (*very high* confidence).

6.2 Country Description

Kiribati is located near the equator in the central Pacific Ocean. The country consists of 32 low lying atolls and one raised limestone island, Banaba, also known as Ocean Island. The islands lie in three main groups which are the Gilbert, Phoenix and Line Islands, listed in sequence from west to east. The islands are located between approximately 5°N–12°S and 168°E–152°W. The distance between the most westerly situated island and the most easterly situated island is about 4000 km. For the most part, the islands are no more that three to four metres above sea level. The total land area is 811 km^2, while the area of the Exclusive Economic Zone is 3.6 million km^2 (Kiribati's First National Communication under the UNFCCC, 1999; Kiribati's National Adaptation Plan of Action, 2007). The estimated 2010 population was 100 835 (Kiribati Country Statistics, SOPAC, 2010) and the capital of Kiribati is South Tarawa in the Gilbert Islands.

Many people in Kiribati, especially away from the main population centre in South Tarawa, rely on a subsistence form of livelihood based on harvesting tree crops and marine resources. The main exports are copra and fish (Ministry of Environment and Social Development, 1999).

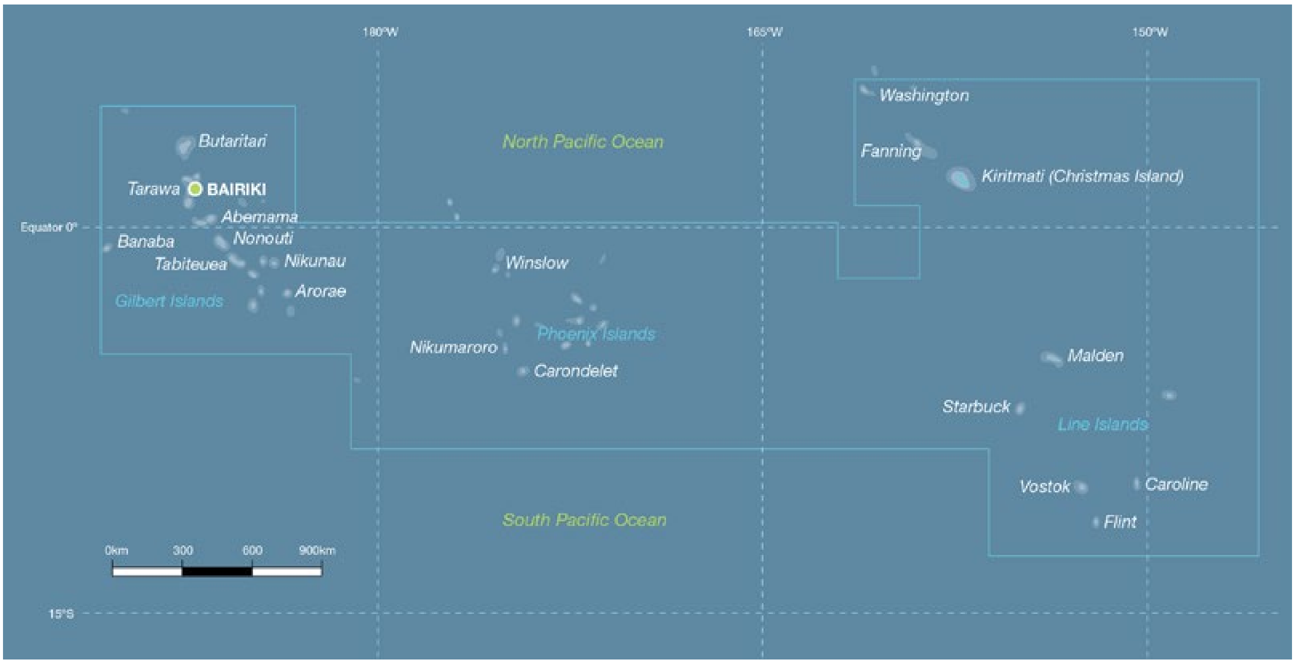

Figure 6.1: Kiribati

6.3 Data Availability

There are currently five operational meteorological stations in Kiribati. Tarawa, the primary station in the Gilbert Islands, is located on the southern side of Tarawa Atoll at Betio. Kiritimati, the primary station in the Line Islands, is situated on the north-west side of the Kiritimati Atoll (Figure 6.1). All five operational stations, including Banaba and Tabuaeran, have rainfall records which began between 1909 and 1945. Banaba has the earliest temperature record which began in 1909 but unfortunately closed in 1993. Tarawa, Beru and Kanton (also known as Canton) have temperature records from 1947. Tarawa and Kiritimati (rainfall only) records from 1950 to 2009 have been used. Both records are homogeneous and more than 95% complete.

Oceanographic records do not cover such a long time period. There are a number of sea-level records available for Kiribati. The best appear to be Tarawa-C (Betio, 1988–2001), Betio (1992–present), Fanning B (1973–1987), Christmas Island (Kiritimati, 1956–1972), Christmas Island II (Kiritimati, 1974–2003), Kanton Island (1949–1974) and Kanton Island-B (1972–2007). A global positioning system instrument to estimate vertical land motion was deployed in Kiribati in 2001 and will provide valuable direct estimates of local vertical land motion in future years. Both satellite (from 1993) and in situ sea-level data (1950–2009; termed reconstructed sea level; Volume 1, Section 2.2.2.2) are available on a global 1° x 1° grid.

Long-term locally-monitored sea-surface temperature data are unavailable for Kiribati, so large-scale gridded sea-surface temperature datasets have been used (HadISST, HadSST2, ERSST and Kaplan Extended SST V2; Volume 1, Table 2.3).

Climate data management training, Kiribati Meteorology Service

6.4 Seasonal Cycles

Kiribati has a hot, humid tropical climate. In Tarawa, average maximum and minimum air temperatures are highly consistent throughout the year, with a range of less than 1°C (Figure 6.2). The air temperatures are very closely related to the sea-surface temperatures. In Kiritimati the seasonal variations in sea-surface temperature are a little higher than near Tarawa, about 1ºC between April, the hottest month, and January, the coolest.

The driest and wettest periods in the year vary from location to location. At Tarawa the driest six-month period begins in June, with the lowest mean rainfall in October. This dry season is called *Aumaiaki* in the local language. The peak of the wet season is in January with a mean of almost 268 mm in that month. The wet season, called *Aumeang* in the local language, usually lasts from around November to April. The highest rainfall during the year usually comes from January to March when the Intertropical Convergence Zone (ITCZ) is furthest south and closest to Tarawa, and to a lesser extent when the South Pacific Convergence Zone (SPCZ) is strongest. The marked change in mean monthly rainfall towards the end of the year is common across Kiribati. Some islands have a slight secondary maximum in July when the ITCZ is most intense, although furthest away to the north. Being over 2000 km to the east, Kiritimati has a different seasonal cycle in rainfall. The wet season is from January to June, with the wettest months being March and April. Rainfall there is affected only by the ITCZ.

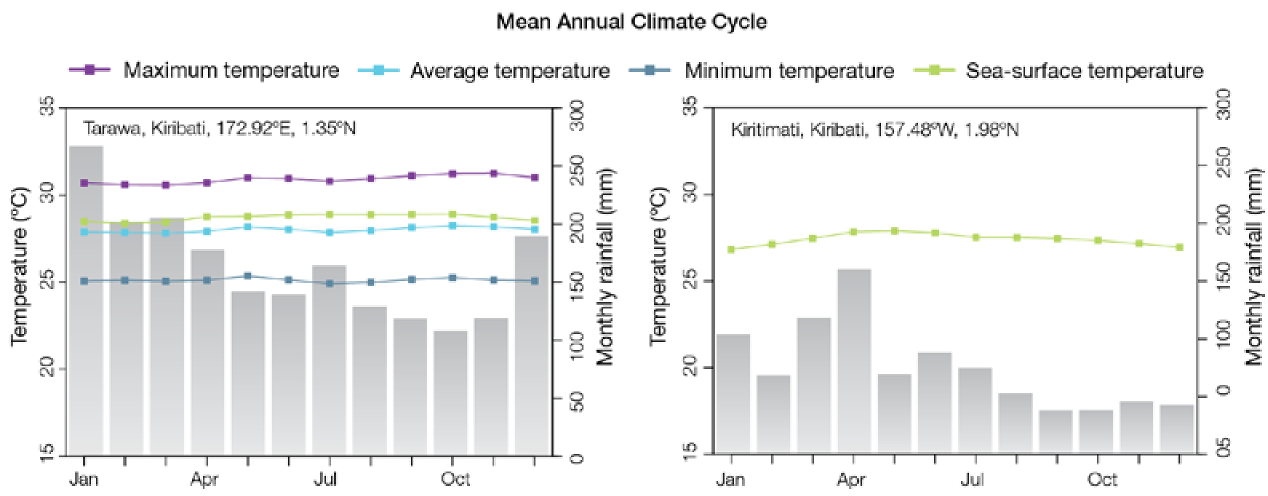

Figure 6.2: Mean annual cycle of rainfall (grey bars) and daily maximum, minimum and mean air temperatures at Tarawa (left), and for rainfall only at Kiritimati (right), as well as local sea-surface temperatures derived from the HadISST dataset (Volume 1, Table 2.3).

6.5 Climate Variability

The climate of Kiribati has high year-to-year variability (Figures 6.3 and 6.4), especially for rainfall. In the driest years, Tarawa received as little as 150 mm, while in the wettest years more than 4000 mm fell. Similar conditions exist in Kiritimati, with huge impacts on water quality and crop production. Most of this year-to-year variability is driven by the El Niño-Southern Oscillation (ENSO; Table 6.1). Many Kiribati islands lie within the equatorial waters that warm significantly during an El Niño event and cool during a La Niña event. As a result rainfall is much higher than normal during an El Niño and much lower during a La Niña. Maximum air temperatures tend to be higher than normal during El Niño years, driven by the warmer oceans surrounding the islands, while in the dry season minimum air temperatures in El Niño years are below normal. ENSO Modoki events (Volume1, Section 3.4.1) have similar impacts to canonical ENSO events, but the influence is only significant on rainfall in the wet season and on maximum air temperatures in both seasons. At Kiritimati, El Niño events also bring wetter conditions in both seasons and La Niña events bring drought.

Table 6.1: Correlation coefficients between indices of key patterns of climate variability and minimum and maximum temperatures (Tmin and Tmax) and rainfall at Tarawa. Only correlation coefficients that are statistically significant at the 95% level are shown.

Climate feature/index		Dry season (May-October)			Wet season (November-April)		
		Tmin	Tmax	Rain	Tmin	Tmax	Rain
ENSO	Niño3.4	-0.31	0.41	0.81		0.53	0.69
	Southern Oscillation Index	0.25	-0.39	-0.74		-0.58	-0.61
Interdecadal Pacific Oscillation Index							
ENSO Modoki Index			0.56			0.57	0.72
Number of years of data		63	60	73	61	61	75

Table 6.2: Correlation coefficients between indices of key patterns of climate variability and minimum and maximum temperatures (Tmin and Tmax) and rainfall at Kiritimati. Only correlation coefficients that are statistically significant at the 95% level are shown.

Climate feature/index		Dry season (May-October)	Wet season (November-April)
ENSO	Niño3.4	0.64	0.67
	Southern Oscillation Index	-0.48	-0.58
Interdecadal Pacific Oscillation Index			
ENSO Modoki Index			
Number of years of data		82	65

6.6 Observed Trends

6.6.1 Air Temperature

Warming trends of a similar magnitude are evident in both annual and seasonal mean air temperatures at Tarawa for 1950–2009. Annual and seasonal minimum air temperature trends are slightly stronger than the trends in maximum air temperatures (Figure 6.3 and Table 6.3).

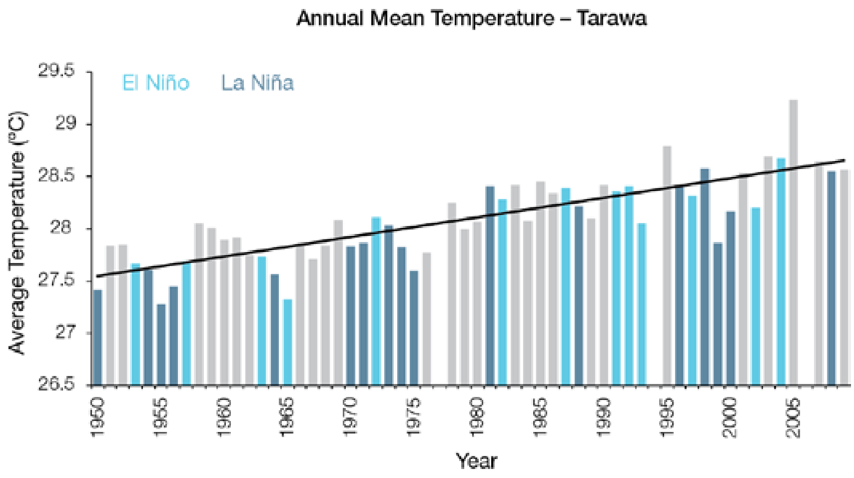

Figure 6.3: Annual mean air temperatures at Tarawa. Light blue, dark blue and grey bars denote El Niño, La Niña and neutral years respectively.

6.6.2 Rainfall

The Kiritimati positive annual rainfall trend for the period 1950–2009 is statistically significant. Annual and seasonal rainfall trends for Tarawa and the seasonal trends for Kiritimati over the same period are not statistically significant (Table 6.3 and Figure 6.4).

Table 6.3: Annual and seasonal trends in maximum, minimum and mean air temperature (Tmax, Tmin and Tmean) and rainfall at Tarawa and rainfall only at Kiritimati for the period 1950–2009. Asterisks indicate significance at the 95% level. Persistence is taken into account in the assessment of significance as in Power and Kociuba (in press). The statistical significance of the air temperature trends is not assessed.

	Tarawa Tmax (°C per 10 yrs)	Tarawa Tmin (°C per 10 yrs)	Tarawa Tmean (°C per 10 yrs)	Tarawa Rain (mm per 10 yrs)	Kiritimati Rain (mm per 10 yrs)
Annual	+0.18	+0.20	+0.19	+60	+115*
Wet season	+0.19	+0.20	+0.19	-15	+60
Dry season	+0.17	+0.20	+0.19	+53	+39

6.6.3 Extreme Events

Droughts, usually associated with La Niña events, are occasionally severe in Kiribati. For example, only 205 mm of rainfall was received over the 18–month period from July 1988 to December 1989, and over the six months from August 1998 to February 1999 total rainfall was only 95 mm. These figures are very much lower than the mean annual rainfall of approximately 2100 mm, and the dry season average of just over 900 mm between May and October.

The recent drought from April 2007 to early 2009 severely affected water supplies in the southern Gilbert Islands and Banaba Island. During this period ground water turned brackish and the leaves of most plants turned yellow. Copra production, the main income source for people in the outer islands, declined. During 1970/71, rainfall suppression was significant across the southern islands of the Gilbert Group. At Kenna on Abemama the drought was severe enough for hardy coconut trees to die.

Tropical cyclones rarely pass within 400 km of the Kiribati Islands. Between 1969/70 and 2009/10 three cyclones passed within 400 km of Arorae Island in western Kiribati and three cyclones within 400 km of Caroline Island in eastern Kiribati. Other important extremes include storm surge and extreme sea levels.

6.6.4 Sea-Surface Temperature

Water temperatures around the Gilbert Island group have risen gradually since the 1950s. Figure 6.7 shows the 1950–2000 sea-surface temperature changes (relative to a reference year of 1990) for the Gilbert Island group region from three different large-scale sea-surface temperature gridded datasets (HadSST2, ERSST and Kaplan Extended SST V2; Volume 1, Table 2.3). Since the 1970s the rate of warming has been approximately 0.15°C per decade. For the Line Island group, historical water temperatures have demonstrated considerable decadal variability. Since the 1970s the rate of warming has been approximately 0.1°C per decade. For the Phoenix Island group water temperatures have risen since the 1950s although considerable decadal variability is evident. Since the 1970s the rate of warming has been approximately 0.12°C per decade. At these regional scales, natural variability plays a large role in determining sea-surface temperatures making it difficult to identify long-term trends.

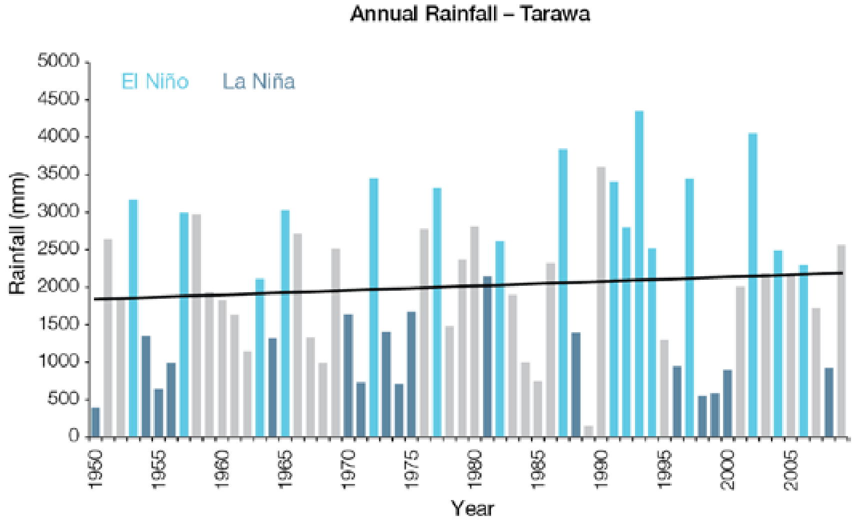

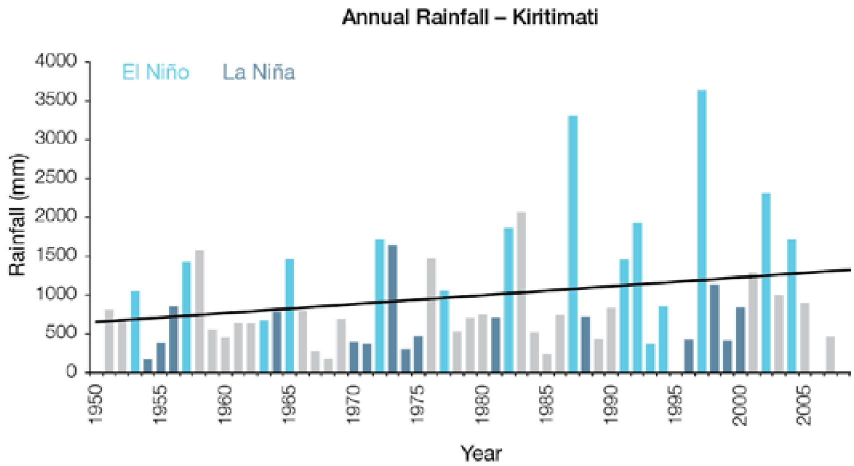

Figure 6.4: Annual rainfall for Tarawa (top) and Kiritimati (bottom). Light blue, dark blue and grey bars denote El Niño, La Niña and neutral years respectively.

6.6.5 Ocean Acidification

Based the large-scale distribution of coral reefs across the Pacific and the seawater chemistry, Guinotte et al. (2003) suggested that seawater aragonite saturation states above 4 were optimal for coral growth and for the development of healthy reef ecosystems, with values from 3.5 to 4 adequate for coral growth, and values between 3 and 3.5, marginal. Coral reef ecosystems were not found at seawater aragonite saturation states below 3 and these conditions were classified as extremely marginal for supporting coral growth.

In the Kiribati region, the aragonite saturation state has declined from about 4.5 in the late 18th century to an observed value of about 3.9 ± 0.1 by 2000.

6.6.6 Sea Level

Monthly averages of the historical tide gauge (since 1950), satellite (since 1993) and gridded sea-level (since 1950) data agree reasonably well after 1993 and indicate year-to-year variability in sea levels of about 26 cm (the estimated 5–95% range) after removal of the seasonal cycle (Figure 6.9). The sea-level rise near Kiribati measured by satellite altimeters (Figure 6.5) since 1993 ranges from 1–4 mm per year, compared with the global average of 3.2 ± 0.4 mm per year. The change is partly linked to a pattern related to climate variability from year to year and decade to decade (Figure 6.9).

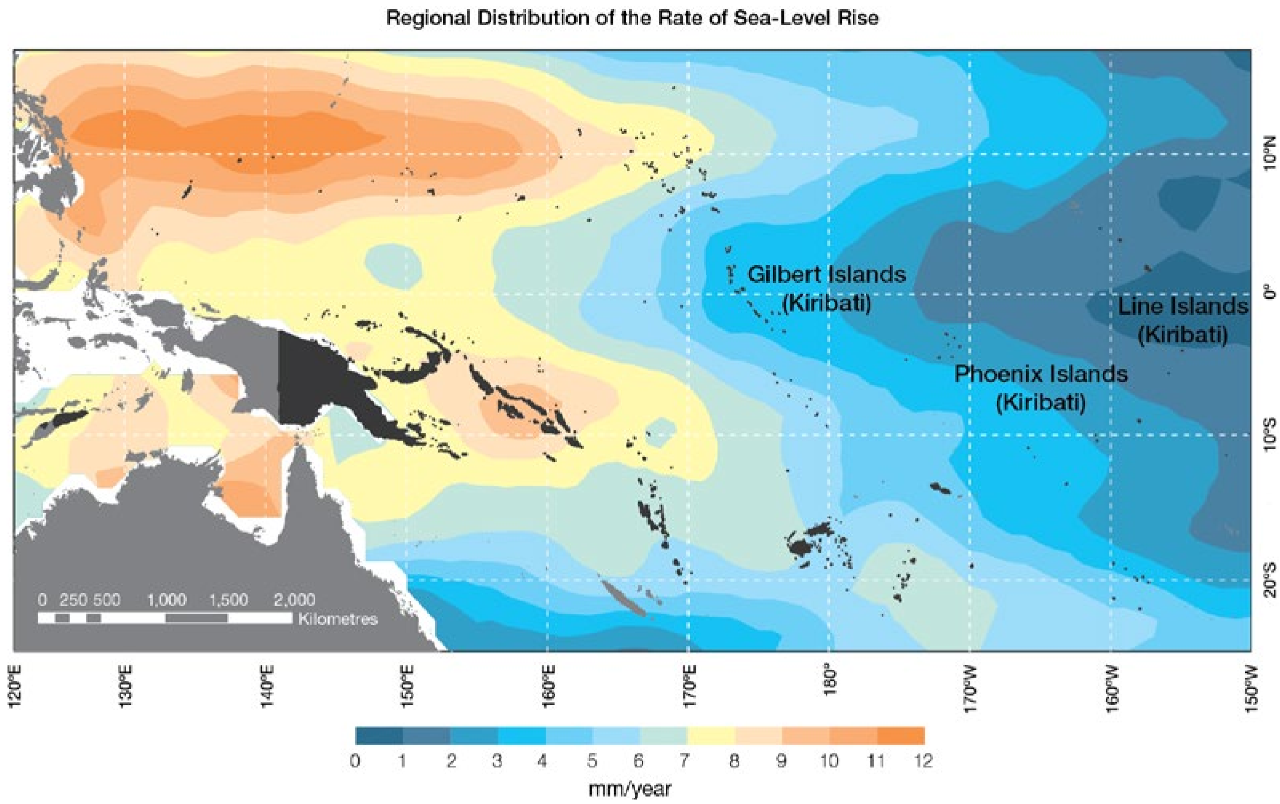

Figure 6.5: The regional distribution of the rate of sea-level rise measured by satellite altimeters from January 1993 to December 2010, with the location of Kiribati indicated. Further detail about the regional distribution of sea-level rise is provided in Volume 1, Section 3.6.3.2.

6.6.7 Extreme Sea-Level Events

The annual climatology of the highest daily sea levels has been evaluated from hourly measurements by tide gauges at Tarawa, Kiritimati and Kanton (Figure 6.6). Highest tides at Tarawa and Kanton are centred on the September equinox, with a secondary peak in February. Kiritimati Island spring tides tend to be greatest near the December solstice. Seasonal and short-term components show relatively little variation throughout the year at all locations, although there is a slight tendency towards higher short-term water levels from November to March at all locations. Sea levels are usually lower in La Niña years and higher during in El Niño years, particularly at Kiritimati. At Kiritimati all of the 10 highest recorded water level events are during El Niño conditions; at Kanton and Tarawa eight and six of the highest occur during El Niño, respectively. These events tend to cluster near the equinoxes at Tarawa and Kanton, and near the December solstice in Kiritimati, indicating that the combination of El Niño conditions and semi-annual tidal variation is the main driver of extreme sea level events, as observed at the respective tidal gauges in Kiribati.

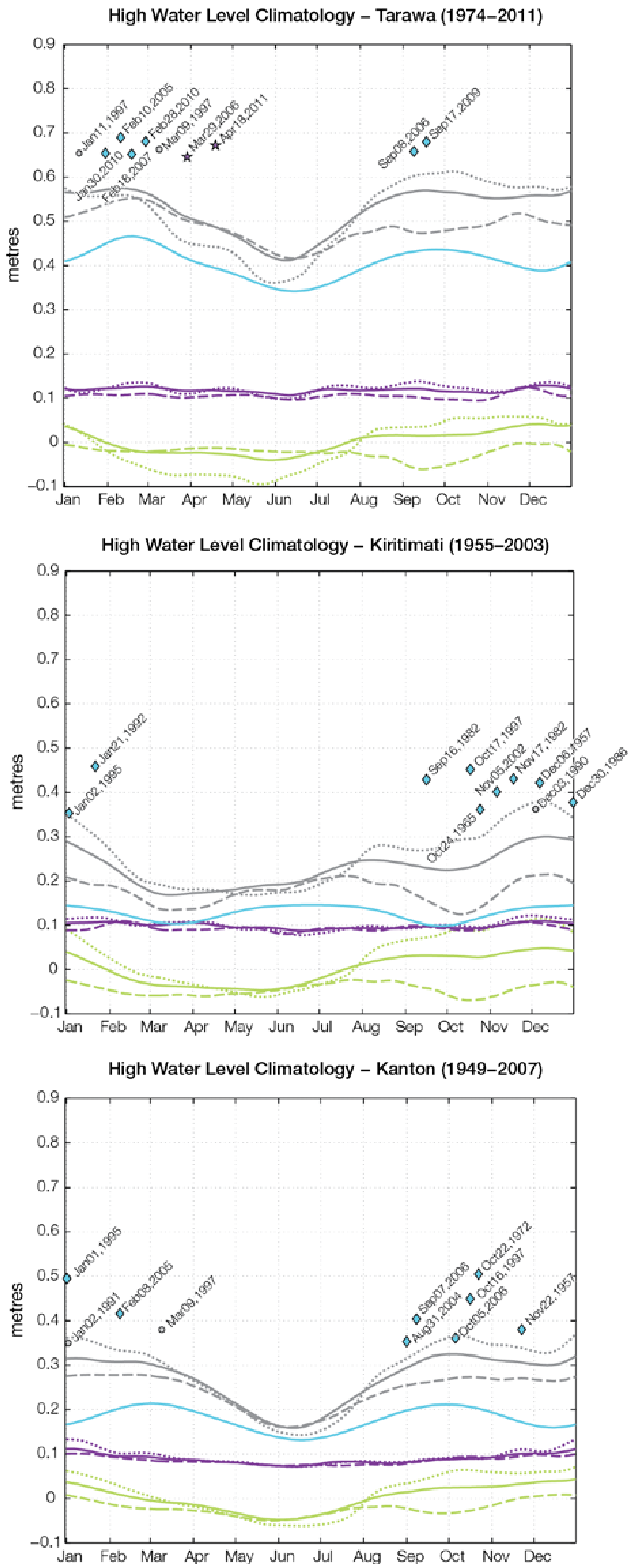

Figure 6.6: The annual cycle of high water relative to Mean Higher High Water (MHHW) due to tides, short-term fluctuations (most likely associated with storms) and seasonal variations for Tarawa (top), Kiritimati (middle) and Kanton (bottom). The tides and short-term fluctuations are respectively the 95% exceedence levels of the astronomical high tides relative to MHHW and short-term sea-level fluctuations. Components computed only for El Niño and La Niña years are shown by dotted and dashed lines, and grey lines are the sum of the tide, short-term and seasonal components. The 10 highest sea-level events in the record relative to MHHW are shown and coded to indicate the phase of ENSO at the time of the extreme event.

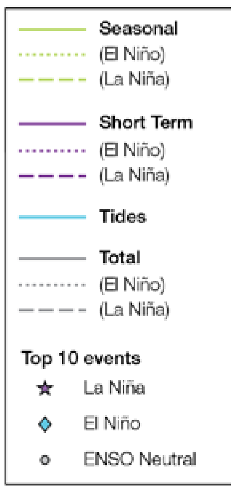

6.7 Climate Projections

Climate projections have been derived from up to 18 global climate models from the CMIP3 database, for up to three emissions scenarios (B1 (low), A1B (medium) and A2 (high)) and three 20-year periods (centred on 2030, 2055 and 2090, relative to 1990). These models were selected based on their ability to reproduce important features of the current climate (Volume 1, Section 5.2.3), so projections from each of the models are plausible representations of the future climate. This means there is not one single projected future for Kiribati, but rather a range of possible futures. The full range of these futures is discussed in the following sections.

These projections do not represent a value specific to any actual location, such as a town or city in Kiribati. Instead, they refer to an average change over the broad geographic region encompassing the islands of Kiribati and the surrounding ocean. Projections refer to the whole of Kiribati unless otherwise stated. In some instances, given that there are some differences between the climate of the Gilbert, Phoenix and Line Island groups (Section 6.4), projections are given separately for these three regions (Figure 1.1 shows the regional boundaries). Section 1.7 provides important information about interpreting climate model projections.

6.7.1 Temperature

Surface air temperature and sea-surface temperature are projected to continue to increase over the course of the 21st century. There is *very high* confidence in this direction of change because:

- Warming is physically consistent with rising greenhouse gas concentrations.
- All CMIP3 models agree on this direction of change.

Almost all of CMIP3 models simulate a slight increase (<1°C) in annual and seasonal mean temperature by 2030, however by 2090 under the A2 (high) emissions scenario temperature increases of greater than 3°C are simulated by the majority of models (Tables 6.4, 6.5 and 6.6). Given the close relationship between surface air temperature and sea-surface temperature, a similar (or slightly weaker) rate of warming is projected for the surface ocean (Figure 6.7). There is *moderate* confidence in this range and distribution of possible futures because:

- There is generally close agreement between modelled and observed temperature trends over the past 50 years in the vicinity of Kiribati, although observational records are limited (Figure 6.7).
- In simulations of the current climate, almost all CMIP3 models have a cold temperature bias in the vicinity of Kiribati (known as the 'cold tongue bias'; Volume 1, Section 5.2.2.1).

Interannual variability in surface air temperature and sea-surface temperature over Kiribati is strongly influenced by ENSO in the current climate (Section 6.5). As there is no consistency in projections of future ENSO activity (Volume 1, Section 6.4.1), it is not possible to determine whether interannual variability in temperature will change in the future. However, ENSO is expected to continue to be an important source of variability for Kiribati and the region.

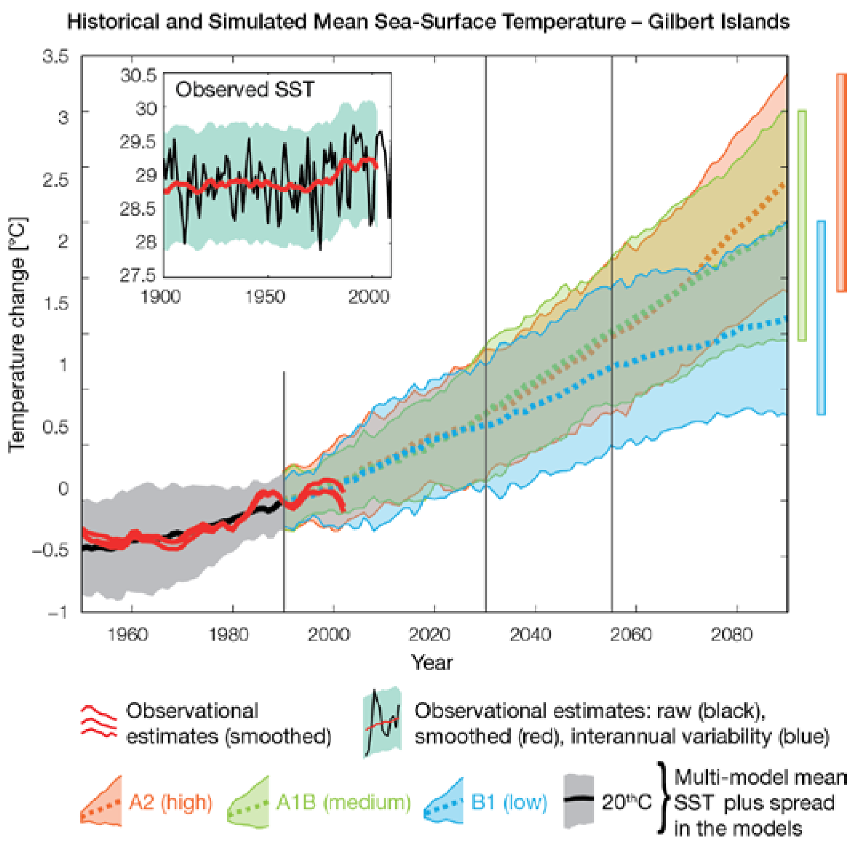

Figure 6.7: Historical climate (from 1950 onwards) and simulated historical and future climate for annual mean sea-surface temperatures (SST) in the region surrounding the Gilbert Islands for the CMIP3 models. Shading represents approximately 95% of the range of model projections (twice the inter-model standard deviation), while the solid lines represent the smoothed (20-year running average) multi-model mean temperature. Projections are calculated relative to the 1980–1999 period (which is why there is a decline in the inter-model standard deviation around 1990). Observational estimates in the main figure (red lines) are derived from the HadSST2, ERSST and Kaplan Extended SST V2 datasets (Volume 1, Section 2.2.2). Annual average (black) and 20-year running average (red) HadSST2 data is also shown inset. Projections for the Phoenix and Line Islands closely resemble those of the Gilbert Islands and are therefore not shown.

6.7.2 Rainfall

Wet season, dry season and annual average rainfall are projected to increase over the course of the 21st century. There is *high* confidence in this direction of change because:

- Physical arguments indicate that rainfall will increase in the equatorial Pacific in a warmer climate (IPCC, 2007; Volume 1, Section 6.4.3).
- Almost all of the CMIP3 models agree on this direction of change.

An increase (>5%) in annual and seasonal mean rainfall is projected by approximately half of the CMIP3 models by as early as 2030, with the majority of models simulating a large increase (>15%) by 2090 (Tables 6.4, 6.5 and 6.6). There is *low* confidence in this range and distribution of possible futures because:

- In simulations of the current climate, almost all CMIP3 models substantially underestimate present day rainfall in the vicinity of Kiribati, in association with the cold tongue bias (Volume 1, Section 5.2.1.2).
- The CMIP3 models are unable to resolve many of the physical processes involved in producing rainfall. As a consequence, they do not simulate rainfall as well as they simulate other variables such as temperature (Volume 1, Chapter 5).

Interannual variability in rainfall over Kiribati is strongly influenced by ENSO in the current climate (Section 6.5). As there is no consistency in projections of future ENSO activity (Volume 1, Section 6.4.1), it is not possible to determine whether interannual variability in rainfall will change in the future.

6.7.3 Extremes

Temperature

The intensity and frequency of days of extreme heat are projected to increase over the course of the 21st century. There is *very high* confidence in this direction of change because:

- An increase in the intensity and frequency of days of extreme heat is physically consistent with rising greenhouse gas concentrations.
- All CMIP3 models agree on the direction of change for both intensity and frequency.

For the Gilbert, Phoenix and Line Islands, the majority of CMIP3 models simulate an increase of approximately 1°C in the temperature experienced on the 1-in-20-year hot day by 2055 under the B1 (low) emissions scenario, with an increase of over 2.5°C simulated by the majority of models by 2090 under the A2 (high) emissions scenario (Tables 6.4, 6.5 and 6.6). There is *low* confidence in this range and distribution of possible futures because:

- In simulations of the current climate, the CMIP3 models tend to underestimate the intensity and frequency of days of extreme heat (Volume 1, Section 5.2.4).
- Smaller increases in the frequency of days of extreme heat are projected by the CCAM 60 km simulations.

Rainfall

The intensity and frequency of days of extreme rainfall are projected to increase over the course of the 21st century. There is *high* confidence in this direction of change because:

- An increase in the frequency and intensity of extreme rainfall is consistent with larger-scale projections, based on the physical argument that the atmosphere is able to hold more water vapour in a warmer climate (Allen and Ingram, 2002; IPCC, 2007). It is also consistent with physical arguments that rainfall will increase in the deep tropical Pacific in a warmer climate (IPCC, 2007; Volume 1, Section 6.4.3).
- Almost all of the CMIP3 models agree on this direction of change for both intensity and frequency.

For the Gilbert, Phoenix and Line Islands, the majority of CMIP3 models simulate an increase of at least 15 mm, 25 mm and 35 mm respectively in the amount of rain received on the 1-in-20-year wet day by 2055 under the B1 (low) emissions scenario, with an increase of at least 40 mm, 65 mm and 80 mm simulated by the majority of models by 2090 under the A2 (high) emissions scenario. The majority of models project that the current 1-in-20-year extreme rainfall event will occur, on average, 5, 10 and 11-12 times per 20-year period by 2055 under the B1 (low) emissions scenario in the Gilbert, Phoenix and Line Islands, respectively. By 2090 under the A2 (high) emissions scenario, the projected frequency increases are 7-8, 18-19 and 22-23 times per 20-year period, respectively. There is *low* confidence in this range and distribution of possible futures because:

- In simulations of the current climate, the CMIP3 models tend to underestimate the intensity and frequency of extreme rainfall (Volume 1, Section 5.2.4), particularly in the vicinity of Kiribati, in association with the cold tongue bias (Volume 1, Section 5.2.1.2).
- The CMIP3 models are unable to resolve many of the physical processes involved in producing extreme rainfall.

Drought

The incidence of drought is projected to decrease over the course of the 21st century. There is *moderate* confidence in this direction of change because:

- A decrease in drought is consistent with projections of increased rainfall (Section 6.7.2).
- The majority of models agree on this direction of change for all drought categories.

For the Gilbert, Phoenix and Line Islands, the majority of CMIP3 models project that mild drought will occur approximately seven to eight times every 20 years in 2030 under all emissions scenarios, decreasing to six to seven times by 2090. The frequency of moderate drought is projected to decrease from two to three times every 20 years in 2030 to once to twice in 2090 for all emissions scenarios, while the majority of CMIP3 models project that severe drought will occur approximately once to twice every 20 years in 2030, decreasing to once every 20 years by 2055 and 2090. There is *low* confidence in this range and distribution of possible futures because:

- There is only low confidence in the range of rainfall projections (Section 6.7.2), which directly influences projections of future drought conditions.

6.7.4 Ocean Acidification

The acidification of the ocean will continue to increase over the course of the 21st century. There is *very high* confidence in this projection as the rate of ocean acidification is driven primarily by the increasing oceanic uptake of carbon dioxide, in response to rising atmospheric carbon dioxide concentrations.

Projections from all analysed CMIP3 models indicate that the annual maximum aragonite saturation state will reach values below 3.5 by about 2045 in the Gilbert Islands, by about 2030 in the Line Islands, and 2055 in the Phoenix Islands. The aragonite saturation will continue to decline thereafter (Figure 6.8; Tables 6.4, 6.5 and 6.6). There is *moderate* confidence in this range and distribution of possible futures because the projections are based on climate models without an explicit representation of the carbon cycle and with relatively low resolution and known regional biases.

The impact of acidification change on the health of reef ecosystems is likely to be compounded by other stressors including coral bleaching, storm damage and fishing pressure.

6.7.5 Sea Level

Mean sea level is projected to continue to rise over the course of the 21st century. There is *very high* confidence in this direction of change because:

- Sea-level rise is a physically consistent response to increasing ocean and atmospheric temperatures, due to thermal expansion of the water and the melting of glaciers and ice caps.
- Projections arising from all CMIP3 models agree on this direction of change.

The CMIP3 models simulate a rise of between approximately 5–15 cm by 2030, with increases of 20–60 cm indicated by 2090 under the higher emissions scenarios (i.e. A2 (high), A1B (medium); Figure 6.9; Tables 6.4, 6.5 and 6.6).

There is *moderate* confidence in this range and distribution of possible futures because:

- There is significant uncertainty surrounding ice-sheet contributions to sea-level rise and a rise larger than projected above cannot be excluded (Meehl et al., 2007b). However, adequate understanding of the processes is currently too limited to provide a best estimate or an upper bound (IPCC, 2007).
- Globally, since the early 1990s, sea level has been rising near the upper end of the above projections. During the 21st century, some studies (using semi-empirical models) project faster rates of sea-level rise.

Interannual variability of sea level will lead to periods of lower and higher regional sea levels. In the past, this interannual variability has been about 23 cm (5–95% range, after removal of the seasonal signal; dashed lines in Figure 6.9 (a)) and it is likely that a similar range will continue through the 21st century. In addition, winds and waves associated with weather phenomena will continue to lead to extreme sea-level events.

In addition to the regional variations in sea level associated with ocean and mass changes, there are ongoing changes in relative sea level associated with changes in surface loading over the last glacial cycle (glacial isostatic adjustment) and local tectonic motions. The glacial isostatic motions are relatively small for the PCCSP region.

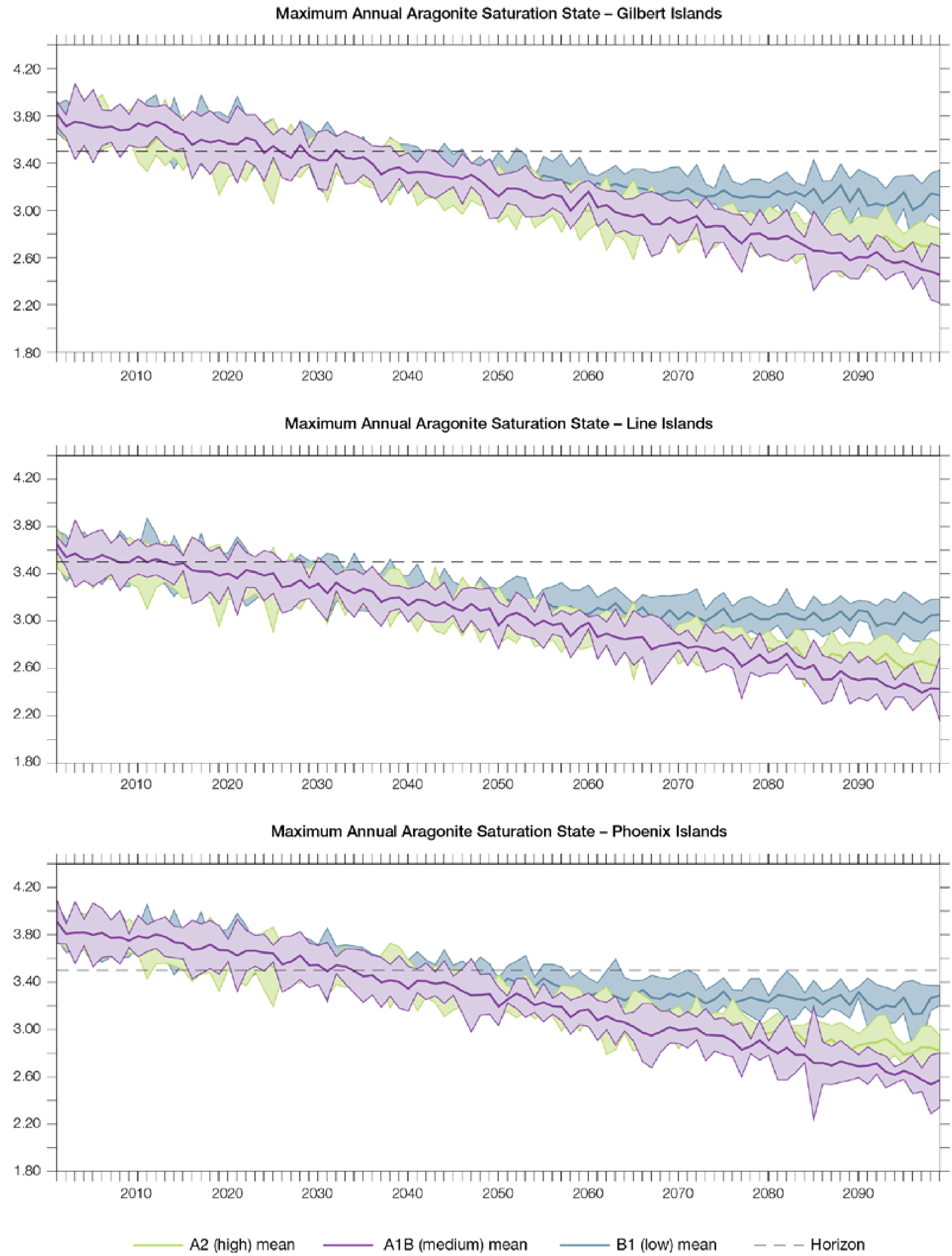

Figure 6.8: Multi-model projections, and their associated uncertainty (shaded area represents two standard deviations), of the maximum annual aragonite saturation state in the sea surface waters of Kiribati (Gilbert Islands, top; the Line Islands, middle; and the Phoenix Islands, bottom) under the different emissions scenarios. The dashed black line represents an aragonite saturation state of 3.5.

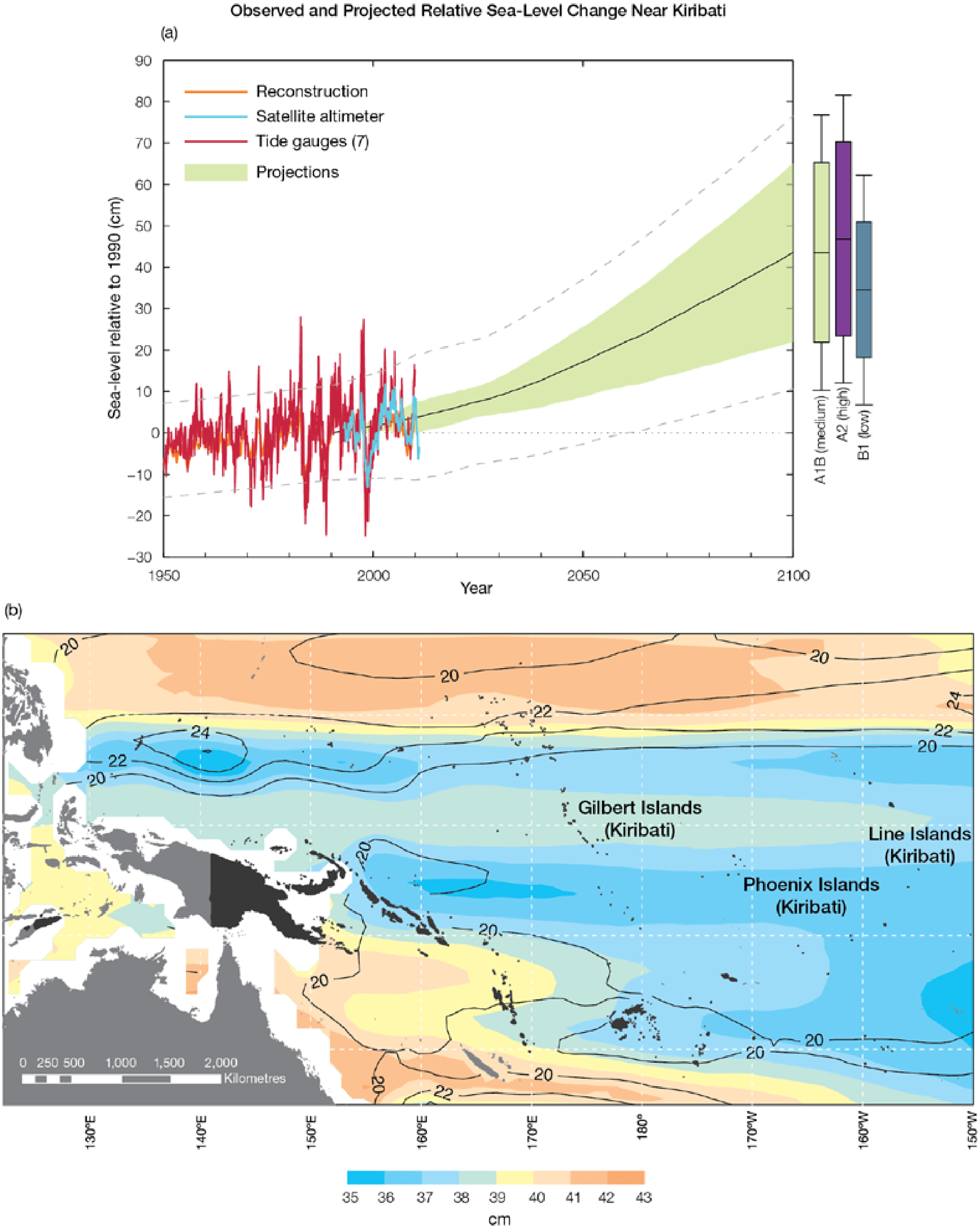

Figure 6.9: Observed and projected relative sea-level change near Kiribati. (a) The observed in situ relative sea-level records are indicated in red, with the satellite record (since 1993) in light blue. The gridded sea level at Kiribati (since 1950, from Church and White (in press)) is shown in orange. The projections for the A1B (medium) emissions scenario (5–95% uncertainty range) are shown by the green shaded region from 1990–2100. The range of projections for the B1 (low), A1B (medium) and A2 (high) emissions scenarios by 2100 are also shown by the bars on the right. The dashed lines are an estimate of interannual variability in sea level (5–95% range about the long-term trends) and indicate that individual monthly averages of sea level can be above or below longer-term averages. (b) The projections (in cm) for the A1B (medium) emissions scenario in the Kiribati region for the average over 2081–2100 relative to 1981–2000 are indicated by the shading, with the estimated uncertainty in the projections indicated by the contours (in cm).

6.7.6 Projections Summary

The projections presented in Section 6.7 are summarised in Table 6.4 (Gilbert Islands), Table 6.5 (Phoenix Islands) and Table 6.6 (Line Islands). For detailed information regarding the various uncertainties associated with the table values, refer to the preceding text in Sections 6.7 and 1.7, in addition to Chapters 5 and 6 in Volume 1. When interpreting the differences between projections for the B1 (low), A1B (medium) and A2 (high) emissions scenarios, it is also important to consider the emissions pathways associated with each scenario (Volume 1, Figure 4.1) and the fact that a slightly different subset of models was available for each (Volume 1, Appendix 1).

Table 6.4: Projected change in the annual and seasonal mean climate for the Gilbert Islands, under the B1 (low; blue), A1B (medium; green) and A2 (high; purple) emissions scenarios. Projections are given for three 20-year periods centred on 2030 (2020–2039), 2055 (2046–2065) and 2090 (2080–2099), relative to 1990 (1980–1999). Values represent the multi-model mean change ± twice the inter-model standard deviation (representing approximately 95% of the range of model projections), except for sea level where the estimated mean change and the 5–95% range are given (as they are derived directly from the Intergovernmental Panel on Climate Change Fourth Assessment Report values). The confidence (Section 1.7.2) associated with the range and distribution of the projections is also given (indicated by the standard deviation and multi-model mean, respectively). See Volume 1, Appendix 1 for a complete listing of CMIP3 models used to derive these projections.

Variable	Season	2030	2055	2090	Confidence
Surface air temperature (°C)	Annual	+0.7 ± 0.5 +0.8 ± 0.6 +0.8 ± 0.5	+1.3 ± 0.6 +1.6 ± 0.7 +1.6 ± 0.6	+1.7 ± 0.7 +2.6 ± 0.9 +3.0 ± 0.8	Moderate
Maximum temperature (°C)	1-in-20-year event	N/A	+1.1 ± 0.6 +1.5 ± 0.6 +1.5 ± 0.6	+1.4 ± 0.9 +2.3 ± 1.3 +2.8 ± 1.5	Low
Minimum temperature (°C)	1-in-20-year event	N/A	+1.4 ± 1.7 +1.7 ± 3.0 +1.5 ± 2.0	+1.8 ± 1.8 +2.6 ± 2.6 +2.8 ± 2.6	Low
Total rainfall (%)*	Annual	+14 ± 25 +12 ± 32 +7 ± 21	+20 ± 37 +23 ± 33 +23 ± 34	+25 ± 36 +37 ± 58 +42 ± 73	Low
Wet season rainfall (%)*	November-April	+10 ± 22 +10 ± 32 +5 ± 25	+14 ± 33 +18 ± 31 +18 ± 40	+19 ± 30 +30 ± 49 +30 ± 59	Low
Dry season rainfall (%)*	May-October	+18 ± 38 +15 ± 42 +12 ± 25	+28 ± 46 +30 ± 49 +31 ± 47	+34 ± 52 +50 ± 84 +57 ± 102	Low
Sea-surface temperature (°C)	Annual	+0.7 ± 0.5 +0.8 ± 0.6 +0.8 ± 0.6	+1.2 ± 0.7 +1.5 ± 0.7 +1.5 ± 0.7	+1.6 ± 0.9 +2.5 ± 1.0 +2.9 ± 1.0	Moderate
Aragonite saturation state (Ωar)	Annual maximum	+3.5 ± 0.2 +3.4 ± 0.2 +3.4 ± 0.2	+3.3 ± 0.1 +3.1 ± 0.2 +3.1 ± 0.1	+3.1 ± 0.2 +2.7 ± 0.2 +2.6 ± 0.2	Moderate
Mean sea level (cm)	Annual	+9 (4–13) +9 (5–14) +9 (5–14)	+17 (9–25) +20 (10–29) +19 (10–28)	+31 (16–45) +38 (19–57) +39 (20–58)	Moderate

*The MIROC3.2(medres) and MIROC3.2(hires) models were eliminated in calculating the rainfall projections, due to their inability to accurately simulate present-day activity of the South Pacific Convergence Zone and the Intertropical Convergence Zone (Volume 1, Section 5.5.1).

Table 6.5: Projected change in the annual and seasonal mean climate for the Phoenix Islands, under the B1 (low; blue), A1B (medium; green) and A2 (high; purple) emissions scenarios. Projections are given for three 20-year periods centred on 2030 (2020–2039), 2055 (2046–2065) and 2090 (2080–2099), relative to 1990 (1980–1999). Values represent the multi-model mean change ± twice the inter-model standard deviation (representing approximately 95% of the range of model projections), except for sea level where the estimated mean change and the 5–95% range are given (as they are derived directly from the Intergovernmental Panel on Climate Change Fourth Assessment Report values). The confidence (Section 1.7.2) associated with the range and distribution of the projections is also given (indicated by the standard deviation and multi-model mean, respectively). See Volume 1, Appendix 1 for a complete listing of CMIP3 models used to derive these projections.

Variable	Season	2030	2055	2090	Confidence
Surface air temperature (°C)	Annual	+0.7 ± 0.5 +0.9 ± 0.5 +0.8 ± 0.4	+1.3 ± 0.6 +1.6 ± 0.6 +1.6 ± 0.5	+1.7 ± 0.7 +2.6 ± 0.9 +3.0 ± 0.7	Moderate
Maximum temperature (ºC)	1-in-20-year event	N/A	+1.0 ± 0.9 +1.5 ± 0.9 +1.5 ± 0.8	+1.4 ± 1.2 +2.2 ± 1.5 +2.8 ± 1.4	Low
Minimum temperature (ºC)	1-in-20-year event	N/A	+1.3 ± 2.0 +1.6 ± 2.3 +1.5 ± 2.1	+2.0 ± 1.8 +2.5 ± 2.2 +2.7 ± 2.3	Low
Total rainfall (%)*	Annual	+14 ± 34 +11 ± 43 +8 ± 21	+18 ± 38 +21 ± 42 +22 ± 41	+22 ± 45 +33 ± 67 +41 ± 76	Low
Wet season rainfall (%)*	November-April	+12 ± 37 +12 ± 64 +6 ± 31	+14 ± 47 +20 ± 49 +20 ± 54	+18 ± 39 +30 ± 74 +36 ± 71	Low
Dry season rainfall (%)*	May-October	+15 ± 35 +13 ± 40 +12 ± 31	+25 ± 48 +28 ± 74 +29 ± 73	+30 ± 72 +42 ± 105 +53 ± 120	Low
Sea-surface temperature (°C)	Annual	+0.7 ± 0.5 +0.8 ± 0.5 +0.8 ± 0.5	+1.2 ± 0.6 +1.5 ± 0.5 +1.5 ± 0.6	+1.6 ± 0.7 +2.5 ± 0.9 +2.8 ± 0.8	Moderate
Aragonite saturation state (Ωar)	Annual maximum	+3.5 ± 0.2 +3.4 ± 0.2 +3.4 ± 0.2	+3.3 ± 0.1 +3.1 ± 0.2 +3.1 ± 0.1	+3.1 ± 0.2 +2.7 ± 0.2 +2.6 ± 0.2	Moderate
Mean sea level (cm)	Annual	+9 (4–13) +9 (5–14) +9 (5–14)	+17 (9–25) +20 (10–29) +19 (10–28)	+31 (16–45) +38 (19–57) +39 (20–58)	Moderate

*The MIROC3.2 (medres) and MIROC3.2(hires) models were eliminated in calculating the rainfall projections, due to their inability to accurately simulate present-day activity of the South Pacific Convergence Zone and the Intertropical Convergence Zone (Volume 1, Section 5.5.1).

Table 6.6: Projected change in the annual and seasonal mean climate for the Line Islands, under the B1 (low; blue), A1B (medium; green) and A2 (high; purple) emissions scenarios. Projections are given for three 20-year periods centred on 2030 (2020–2039), 2055 (2046–2065) and 2090 (2080–2099), relative to 1990 (1980–1999). Values represent the multi-model mean change ± twice the inter-model standard deviation (representing approximately 95% of the range of model projections), except for sea level where the estimated mean change and the 5–95% range are given (as they are derived directly from the Intergovernmental Panel on Climate Change Fourth Assessment Report values). The confidence (Section 1.7.2) associated with the range and distribution of the projections is also given (indicated by the standard deviation and multi-model mean, respectively). See Volume 1, Appendix 1 for a complete listing of CMIP3 models used to derive these projections.

Variable	Season	2030	2055	2090	Confidence
Surface air temperature (°C)	Annual	+0.7 ± 0.5 +0.8 ± 0.5 +0.8 ± 0.4	+1.2 ± 0.6 +1.6 ± 0.6 +1.5 ± 0.5	+1.7 ± 0.7 +2.5 ± 0.9 +2.9 ± 0.6	Moderate
Maximum temperature (°C)	1-in-20-year event	N/A	+1.1 ± 0.8 +1.5 ± 0.9 +1.6 ± 0.9	+1.5 ± 1.1 +2.2 ± 1.5 +2.9 ± 1.3	Low
Minimum temperature (°C)	1-in-20-year event	N/A	+1.3 ± 2.0 +1.7 ± 2.2 +1.5 ± 2.1	+1.9 ± 2.0 +2.5 ± 2.6 +2.6 ± 2.2	Low
Total rainfall (%)*	Annual	+9 ± 22 +9 ± 30 +6 ± 19	+11 ± 22 +14 ± 38 +13 ± 40	+14 ± 33 +19 ± 49 +23 ± 53	Low
Wet season rainfall (%)*	November-April	+9 ± 22 +9 ± 35 +6 ± 23	+9 ± 25 +13 ± 38 +13 ± 41	+13 ± 30 +17 ± 45 +19 ± 41	Low
Dry season rainfall (%)*	May-October	+8 ± 23 +8 ± 26 +6 ± 18	+12 ± 22 +15 ± 38 +13 ± 41	+16 ± 35 +21 ± 53 +26 ± 68	Low
Sea-surface temperature (°C)	Annual	+07 ± 0.4 +0.8 ± 0.5 +0.7 ± 0.4	+1.1 ± 0.5 +1.5 ± 0.6 +1.4 ± 0.6	+1.6 ± 0.7 +2.4 ± 0.9 +2.7 ± 0.7	Moderate
Aragonite saturation state (Ωar)	Annual maximum	+3.5 ± 0.2 +3.4 ± 0.2 +3.4 ± 0.2	+3.3 ± 0.1 +3.1 ± 0.2 +3.1 ± 0.1	+3.1 ± 0.2 +2.7 ± 0.2 +2.6 ± 0.2	Moderate
Mean sea level (cm)	Annual	+9 (4–13) +9 (5–14) +9 (5–14)	+17 (9–25) +20 (10–29) +19 (10–28)	+31 (16–45) +38 (19–57) +39 (20–58)	Moderate

*The MIROC3.2 (medres) and MIROC3.2(hires) models were eliminated in calculating the rainfall projections, due to their inability to accurately simulate present-day activity of the South Pacific Convergence Zone and the Intertropical Convergence Zone (Volume 1, Section 5.5.1).